THE ASTROPHYSICAL JOURNAL, 262:1–8, 1982 November 1

EVOLUTION OF THE CLUSTER X-RAY LUMINOSITY FUNCTION SLOPE

J. PATRICK HENRY, ANDRZEJ SOLTAN[1], AND ULRICH BRIEL
Harvard-Smithsonian Center for Astrophysics

AND

JAMES E. GUNN
Princeton University Observatory
Received 1981 August 3; accepted 1982 April 28

ABSTRACT

We report the results of an X-ray survey of 58 clusters of galaxies at moderate and high redshifts. Using a luminosity-limited subsample of 25 objects, we find that to a redshift of 0.5 the slope (i.e., power-law index) of the luminosity function of distant clusters is independent of redshift and consistent with that of nearby clusters. The time scale for change in the slope must be greater than 9 billion years. We cannot measure the normalization of the luminosity function because our sample is not complete. We discuss the implications of our data for theoretical models. In particular, Perrenod's models with high Ω are excluded by the present data.

Subject headings: cosmology — galaxies: clusters of — galaxies: evolution — luminosity function — X-rays: sources

I. INTRODUCTION

The epochs at which galaxies and clusters formed and their evolutionary time scales are not known with certainty. Some previous studies have indicated that individual galaxies in clusters have changed substantially from the epoch corresponding to a redshift of about 0.5 to the present. Butcher, Oemler, and Wells (1980) have observed a number of high-redshift ($z = 0.2$–0.5), centrally condensed clusters and found that they contained a large population of blue objects, presumably spiral galaxies. The number of these objects is in excess of that observed in similar clusters at low redshift. However, not all high-redshift clusters show this effect (Koo 1981), and it is not confirmed for 3C 295 (Mathieu and Spinrad 1981). Katgert, de Ruiter, and van der Laan (1979) have shown that the radio galaxy population, consisting of elliptical galaxies, evolves quite strongly beyond $z \approx 0.25$ such that the proper density is enhanced by a factor of ~ 30 at $z \approx 0.5$ relative to the present epoch. These observations indicate that several different properties of individual galaxies may evolve on a time scale of 1×10^9 yr. However, the observed time scales for color evolution of first-ranked cluster galaxies are of order 10×10^9 yr. Kristian, Sandage, and Westphal (1978) show that the observed $B-V$ and $V-R$ colors of these galaxies follow that expected of a redshifted elliptical galaxy to within 0.2 mag out to a redshift of ~ 0.5, and Lebofsky (1981) has done the same for $H-K$ colors to a limit of 0.4 mag to a redshift of ~ 1. Spinrad, Stauffer, and Butcher (1981) have shown that the rest frame UV colors of two radio galaxies at a redshift of 1.1 are only 0.7 mag bluer than local giant elliptical galaxies. Of course, there is no reason to expect that any of these time scales would be the same, since they are for different physical processes.

The detection of X-ray emission from distant clusters of galaxies (Henry *et al.* 1979; Ulmer *et al.* 1981; Perrenod and Henry 1981; and the present results) provides new observational material for the study of cluster evolution. The time scale of the cluster luminosity evolution will reflect the time required for the gas to collect and heat in the steepening cluster potential. Thus the time scale that we measure may be similar to that observed by Butcher, Oemler, and Wells (1980), which reflects the gas loss from the cluster galaxies, presumably the source of the X-ray gas.

Perrenod (1980) has made detailed calculations of the evolution of the cluster X-ray luminosity function (XLF). These calculations assume that galaxies form first and then cluster. A cluster mass function is calculated assuming a Gaussian distribution of density enhancements for a given mass scale, and then the cluster luminosity function is calculated from this assuming a power-law relation between mass and X-ray luminosity. Perrenod calculates a short time scale ($\sim 10^9$ yr) for the evolution of the XLF for large Ω ($=2\ q_0$) and decreasingly slower evolution for decreasingly smaller Ω. This reflects the fact that collapse of density inhomogeneities proceeds more slowly after $1 + z \approx \Omega^{-1}$ (cf. Fall 1979).

In a previous paper (Henry *et al.* 1979), we tried to compare the luminosity of individual clusters at high z with that of an appropriate sample of low-z clusters. The low-z sample was composed of objects likely to have evolved from clusters similar to those observed at high z. Although this procedure is subject to many systematic

[1] On leave from N. Copernicus Astronomical Center, Warsaw, Poland.

errors, we adopted it because we had a very small sample and also because the available model calculations were done for single evolving clusters. The results were consistent with models predicting an increasing cluster luminosity with time. We could not prove that those models were correct because, with a large spread in luminosity for any given class of cluster (cf. McHardy 1978; Jones and Forman 1978; McKee *et al.* 1980), the observed objects at high z could merely not be average members of their class.

We now have a substantially larger sample. With this sample we can start to make quantitative measurements of cluster X-ray luminosity evolution. The clusters that we have observed are chosen from the literature and for the most part reflect only those clusters with redshifts published as of 1978. Our sample is sufficiently large that we can estimate the slope of the XLF as a function of z. (If the XLF $\propto L^{-\beta}$, then we define the slope to be β.) This method eliminates the need of trying to guess into what type of object a given high-z cluster will evolve. However, we cannot measure the XLF normalization because our sample is incomplete. We find that, at least up to $z \approx 0.5$, the slope of the XLF does not change; the 2 σ limit on the time scale for changes is greater than 9×10^9 yr. We also compare our data with the predictions of Perrenod's (1980) models and find that high Ω models are excluded. The time scale for change of the characteristic cluster luminosity is again greater than 9×10^9 yr (2 σ). Ulmer *et al.* (1981) also find no evolution of the cluster XLF (both slope and normalization) to $z \approx 0.18$, but they place no quantitative limits on possible variations.

II. OBSERVATIONS

The observations presented here were made using the Imaging Proportional Counter at the focus of the *Einstein Observatory* X-ray telescope. A list of the observed clusters is given in Table 1 in order of increasing redshift. For completeness we included objects published previously (Henry *et al.* 1979). Columns (1) and (2) of Table 1 are self-explanatory. Columns (3), (4), and (5) give the source count rate, observed energy band, and exposure time, respectively. The observed (at Earth) flux density at 2 keV (in the cluster frame) and the luminosity in the energy band of 0.5–4.5 keV at the cluster are given in columns (6) and (7), assuming $H_0 = 50$ km s^{-1} Mpc^{-1} and $\Omega = 0$. These values are assumed throughout. One sigma errors on the count rate, flux density, and luminosity are given below the values of these quantities in the table. The procedure used for the flux and luminosity determination and some details of the data reduction are given in Henry *et al.* (1979). Briefly, all sources were assumed to have the same standard spectrum, which was thermal bremsstrahlung with temperature of 7 keV at the cluster and low energy absorption in our Galaxy due to a hydrogen column density of 3×10^{20} cm^{-2}. The errors in Table 1 are calculated using Poisson statistics and do not include errors introduced by the standard spectrum assumption and absolute calibration uncertainties. We estimate that both of these sources together cause no more than a 30% error in the flux. All detected sources are detected at greater than 5 σ, even though some of the luminosities are measured to less precision than this. If the temperatures of distant clusters are cooler than nearby ones, as claimed by Perrenod and Henry (1981), our assumption of a constant temperature of 7 keV would be incorrect. However, the derived luminosity and flux density differ by about 10% from that given in Table 1 when the assumed temperature is lowered by a factor of 2.

Detailed HRI observations of A2218, one of the clusters in Table 1, have been reported by Boynton *et al.* (1982). The detection of four of the clusters in Table 1 has been previously reported in the literature. They are (with the previous 2–10 keV luminosities in units of 10^{44} ergs s^{-1}, adjusted to $H_0 = 50$ km s^{-1} Mpc^{-1} where necessary) A586 (25.6 ± 0.2), A1413 (11.7 ± 0.2), A2244 (13.1 ± 1.0) (Ulmer *et al.* 1980, 1981), and A1146 (22.5 ± 2.4) (McHardy 1978; Pravdo *et al.* 1979). Except for A1413, the luminosity reported here is a factor of 5–10 lower than that given previously. This discrepancy is probably due to misidentifications of the X-ray sources detected by the large-beam nonimaging detectors used in the earlier work.

III. EVOLUTION OF THE LUMINOSITY FUNCTION SLOPE

In this section we discuss our data without reference to any specific model. The advantage of this approach is that any conclusions we reach are dependent only on the quality of the data. The disadvantage is that the conclusions that can be drawn are weak.

The clusters listed in Table 1 were selected from various optical and radio surveys and do not constitute a statistically complete sample. Correlation of richness, Rood-Sastry class, and Bautz-Morgan class with the X-ray luminosity (or its upper envelope) (Bahcall 1977; Jones and Forman 1978; McHardy 1978; McKee *et al.* 1980) introduces bias to our X-ray data. To minimize these effects, one should divide the available material into subsamples according to richness and Bautz-Morgan class. This is not feasible at present for two reasons. First, a much larger sample is required to improve statistics; second, high-redshift clusters are too faint to be properly classified. We adopted the less direct approach of determining the slope (i.e., power-law index) of the XLF for different redshift bins. This parameterization is justified because, for luminosities between $\sim 3 \times 10^{43}$ and $\sim 3 \times 10^{45}$ ergs s^{-1}, the low-z XLF can be well approximated by the power law $N(L_x) = N_0 L_x^{-\beta}$ (McKee *et al.* 1980; Piccinotti *et al.* 1982). There is an indication that the slope of the XLF steepens above 3×10^{45} ergs s^{-1} (Schwartz 1978). Furthermore, the slope is a parameter of the XLF which seems to be the least influenced by various selection effects. This may be illustrated by the apparently similar slope of the XLF of Abell clusters for richness classes 0, 1, and 2 in Figure 3 of McHardy (1978).

We estimated the slope of the XLF by means of the maximum-likelihood method (Crawford, Jauncey, and

TABLE 1

X-RAY PROPERTIES OF DISTANT CLUSTERS OF GALAXIES

Name (1)	z (2)	Rate (s^{-1}) (3)	Band (keV) (4)	Time (s) (5)	F_E (2 keV/[1 + z]) (keV cm^{-2} s^{-1} keV^{-1}) (6)	L_x (0.5–4.5 keV) (ergs s^{-1}) (7)
A98	0.1028	7.6E−2	0.20–2.70	2079	3.6E−4	1.7E44
		1.2			0.5	0.2
A2244	0.104:	8.0E−2	0.20–4.24	2019	8.8E−4	2.6E44*
		1.0			1.1	0.3
A795	0.1361	1.6E−1	0.34–4.40	851	7.7E−4	3.8E44*
		0.2			0.8	0.4
A2240	0.137	<5.2E−3	0.33–4.30	3093	<2.6E−5	<1.3E43
A1146	0.137	8.0E−2	0.28–4.25	1185	3.8E−4	1.9E44*
		1.2			0.5	0.3
A46	0.140	3.8E−2	0.26–4.02	1477	1.8E−4	9.4E43
		0.8			0.4	2.0
A1413	0.1426	3.9E−1	0.29–4.40	2549	1.9E−3	1.0E45*
		0.1			0.1	0.04
A1674	0.155:	4.4E−4	0.24–4.67	578	1.3E−4	8.7E43
		1.7			0.5	3.4
A2009	0.157:	3.0E−1	0.19–4.80	3712	1.4E−3	9.5E44*
		0.1			0.1	0.3
A31	0.159	3.9E−2	0.25–2.90	1802	2.1E−4	1.4E44
		0.8			0.4	0.3
A588	0.160	8.6E−3	0.20–4.79	11,722	7.5E−5	5.2E43
		1.8			1.6	1.1
A2218	0.171	1.7E−1	0.32–4.30	2942	8.1E−5	6.5E44*
		0.1			0.5	0.4
A586	0.172	1.5E−1	0.26–4.02	1840	7.4E−4	5.9E44*
		0.1			0.5	0.4
Cl 0025+062	0.180	<3.4E−4	0.26–4.02	2233	<3.0E−5	<2.7E43
A1954	0.181	2.4E−2	0.21–4.42	1742	1.4E−4	1.2E44
		0.6			0.3	0.3
A864	0.185:	4.1E−3	0.22–4.45	2274	2.5E−5	2.3E43
		2.4			1.5	1.3
A801	0.1917	4.2E−2	0.19–4.64	1486	1.9E−4	1.9E44*
		0.8			0.4	0.4
A115	0.1959	1.8E−1	0.29–2.40	2339	9.1E−4	1.1E45*
		0.1			0.5	0.1
A732	0.202	5.8E−2	0.19–4.64	5662	2.7E−4	2.9E44*
		0.4			0.2	0.2
A223(A, B)	0.207	2.3E−2	0.28–4.22	1079	1.3E−4	1.5E44
		0.9			0.5	0.6
A963	0.207	1.5E−1	0.36–4.50	782	7.8E−4	9.1E44*
		0.2			0.8	1.0
A1246	0.216	1.2E−1	0.19–4.67	1739	5.9E−4	7.4E44*
		0.1			0.5	0.7
A222	0.217	5.7E−2	0.28–4.22	1079	2.9E−4	3.7E44*
		1.0			0.5	0.7
A2111	0.228	9.2E−2	0.17–4.51	2247	4.6E−4	6.5E44*
		0.9			0.5	0.7
A1952	0.247	1.7E−2	0.21–4.42	1742	8.3E−5	1.4E44
		0.5			2.6	0.4
ZwC 1545+21	0.270	1.4E−4	0.24–3.89	4684	4.6E−5	9.1E43
		0.4			1.3	2.6
Cl 11328+31	0.270	<7.5E−3	0.32–4.70	1643	<4.1E−5	<8.0E43
A348	0.274	1.9E−2	0.28–4.20	2969	9.7E−5	2.0E44*
		0.4			2.1	0.4
A41	0.279	3.6E−2	0.26–4.08	1046	1.8E−4	3.9E44*
		0.8			0.4	0.8
Cl 0819+54	0.307	<2.0E−3	0.27–4.12	3200	<1.0E−5	<2.6E43
A2444	0.324	<5.3E−3	0.20–4.50	6051	<2.7E−5	<7.7E43
A1525	0.325	<7.2E−3	0.22–3.59	1629	<3.8E−5	<1.1E44
Cl 2244−02	0.328	9.8E−3	0.33–4.32	4401	5.1E−5	1.5E44
		3.0			1.5	0.4
A895	0.360	<6.7E−3	0.32–4.29	1783	<3.5E−5	<1.3E44
A913	0.366:	2.2E−2	0.33–4.32	6126	1.2E−4	4.3E44*
		0.2			0.1	0.4
3C 268.3	0.371	<6.4E−3	0.33–4.36	2175	<3.4E−5	<1.3E44

TABLE 1—*Continued*

Name (1)	z (2)	Rate (s^{-1}) (3)	Band (keV) (4)	Time (s) (5)	F_E (2 keV/[1 + z]) (keV cm^{-2} s^{-1} keV^{-1}) (6)	L_x (0.5–4.5 keV) (ergs s^{-1}) (7)
A370	0.373	4.9E−2	0.23–4.16	3943	2.5E−4	9.7E44*
		0.6			0.3	1.0
Cl 0822+67	0.384	<5.8E−3	0.33–4.32	1853	<3.1E−5	<1.3E44
Cl 0949+44	0.385	<3.9E−4	0.20–4.31	3725	<2.7E−5	<1.1E44
Cl 0024+16	0.390	1.3E−2	0.22–4.04	16,640	6.5E−5	2.7E44*
		0.2			0.1	0.4
A908	0.390:	1.1E−2	0.21–4.42	4837	1.1E−4	4.7E44*
		0.2			0.2	0.9
Cl 1613+31	0.415	3.1E−3	0.16–4.04	18,569	1.6E−5	7.5E43
		0.8			0.5	2.1
Cl 0303+17	0.450	9.5E−3	0.23–4.60	15,585	5.0E−5	2.8E44*
		2.1			1.1	0.6
3C 200	0.458	4.5E−3	0.36–4.55	6173	2.5E−5	1.5E44
		2.3			1.3	0.7
3C 295	0.461	2.8E−2	0.32–4.35	13,463	1.5E−4	9.2E44*
		0.2			0.1	0.8
3C 19	0.482	9.8E−3	0.20–4.27	11,990	5.2E−5	3.4E44*
		2.0			1.0	0.7
Cl 0312+14	0.510	<2.8E−3	0.17–4.28	13,659	<1.5E−5	<1.1E44
Cl 1600+41	0.540	<3.3E−3	0.18–4.21	10,907	<1.9E−5	<1.6E44
Cl 0016+16	0.545	5.3E−2	0.22–4.49	5591	2.9E−4	2.5E45*
		0.4			0.2	0.2
3C 330	0.549	<2.4E−3	0.20–2.70	7448	<1.6E−5	<1.2E44
Cl 2142+03	0.550	<2.3E−3	0.36–4.51	13,612	<1.3E−5	<1.2E44
PKS 0116+08	0.5936	7.8E−3	0.20–4.60	8321	5.1E−5	5.1E44*
		1.6			1.1	1.1
Cl 1558+41	0.580	<3.9E−3	0.18–4.85	4625	<2.3E−5	<2.2E44
Cl 2155+03	0.660	<2.5E−3	0.18–4.63	15,268	<1.4E−5	<1.8E44
3C 343.1	0.750	3.2E−3	0.25–4.40	3478	2.1E−5	3.4E44
		1.4			0.9	1.5
3C 318	0.752	3.8E−3	0.27–4.23	39,970	2.0E−5	3.4E44
		1.1			0.6	1.0
3C 6.1	0.840	3.1E−3	0.20–4.26	13,359	1.9E−5	3.9E44
		1.0			0.6	1.3
3C 184	0.99	<3.0E−3	0.20–4.79	11,722	<2.0E−5	<5.9E44

NOTE.—Clusters 0303+17, 0312+14, 1558+41, 1600+41, 2142+03, and 2155+03 are from an optically selected sample of J. E. Gunn and J. B. Oke (in preparation). The luminosity of 0024+16 is from Helfand, Ku, and Abramopoulos 1980. Clusters have been detected around 3C 200 (Schild, private communication), 3C 6.1, and 3C 184 (Gunn, private communication) on deep CCD pictures taken at the MMT and the Hale 5 m telescope, respectively. Clusters with luminosities marked with an asterisk form the statistical sample. One keV cm^{-2} s^{-1} keV^{-1} = 6.63 × 10^{-4} Jy.

Murdoch 1970). Murdoch, Crawford, and Jauncey (1973) have shown that this technique is sensitive to the observational errors for large errors. For example, a minimum signal-to-noise ratio of 5 is required to accurately determine the number–flux density relation. By an argument similar to that in Murdoch *et al.*, we find that for our case a minimum signal-to-noise ratio of 4 is acceptable because the XLF slope is flatter than the standard differential source counts. (In fact, the minimum signal-to-noise ratio in the luminosity determination of our final sample is 4.6; see below.)

Following Lightman, Hertz, and Grindlay (1980), we have generalized the likelihood function of Murdoch *et al.* to include measurement errors which vary from object to object in the sample. Murdoch *et al.* assumed each object in the sample had the same error. To do this we introduced the error distribution $g(l_i, L, \sigma_i)$, which is the probability that a source with true luminosity L will be detected with luminosity l_i, where σ_i is a standard deviation of the ith luminosity measurement. In the present calculations we assumed Gaussian error distribution. The likelihood function is then given by

$$L_k(\beta) = \prod_{i=1}^{J} \frac{\int_0^\infty dL L^{-\beta} g(l_i, L, \sigma_i)}{\int_{L_{kth}}^\infty dl \int_0^\infty dL L^{-\beta} g(l, L, \sigma_i)}, \qquad (1)$$

where J is the number of clusters in the analyzed sample, and L_{kth} is the appropriate threshold luminosity for the kth redshift range as defined below. In practice it is convenient to use the function $S_k = -2 \ln L_k$ rather than L_k itself. Minimization of S_k provides the estimate of the slope β. The uncertainty range is determined according to the method described in Cash (1979) and Avni *et al.* (1980). That is, if there are q "interesting" parameters, then S_k has a χ^2 distribution with q degrees of freedom so that pth confidence level is given by

$$S_k = S_k^{\min} + \chi_q^2(p) . \qquad (2)$$

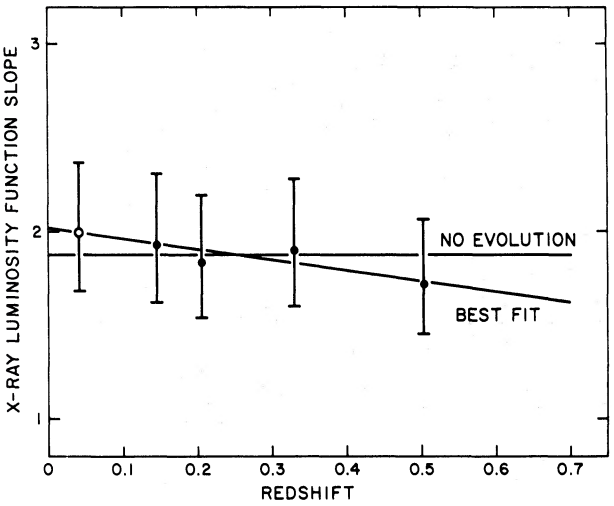

FIG. 1.—The slope of the cluster X-ray luminosity function vs. redshift. The data are plotted at the average redshift of each bin; filled circles are the data from this paper, the open circle is the data from McKee *et al.* (1980). The best fit straight line of the form $\beta = a + bz$ is indicated.

The exposure times of our observations were adjusted so that luminosities could be measured at the 4 σ level for all clusters above $L_{kth} = 1.75 \times 10^{44}$ ergs s^{-1} for redshifts between 0.1 and 0.5. For the redshift range 0.5–0.6, the 4 σ threshold luminosity was 2.4×10^{44} ergs s^{-1}. From Table 1 we selected objects above the given threshold and divided them into four redshift bins ($k = 1$ to 4 inclusive): $0.1 < z < 0.18$ (7), $0.18 < z < 0.22$ (6), $0.22 < z < 0.40$ (7), and $0.40 < z < 0.6$ (5). The numbers in parentheses are the numbers of clusters in each bin. Then the value of β which minimized S_k was found, and 1 σ errors were determined by setting $\chi_q^2(p) = 1$ in equation (2). The results are plotted in Figure 1 and tabulated in Table 2.

There are two comments that should be made about our procedure for estimating β and its error. The error σ_i on the ith luminosity measurement l_i is a function of l_i. This dependence, which should be included when performing the l-integral in the denominator of equation (1), is proportional to $\{N_s + [1 + (A_s/A_B)^2]N_B\}^{1/2}$, where N_s is the number of source counts, N_B is the number of background counts in the source region, and A_s/A_B is the ratio of the area on the detector used to determine the source counts to that used to determine the background counts. We have not included this dependence when performing the integrals in equation (1). It is clear that, if $N_B \gg N_s$ (background-limited case), then there is no l_i dependence. For our observations, σ_i changes by less than $\pm 10\%$ as l_i changes by $\pm 4\ \sigma_i$. Since the integral in the denominator of equation (1) is negligible outside this range, we expect that our neglect of the l_i dependence of σ_i will have little impact on our results. We have verified numerically that this is true in the limiting cases where $N_B = 0$ and where $\sigma_i = 0$. Indeed, we feel that the latter

TABLE 2

X-RAY CLUSTER LUMINOSITY FUNCTION SLOPE

Redshift Range	$\beta(z)$
0.10–0.18	$1.92^{+0.39}_{-0.30}$
0.18–0.22	$1.83^{+0.37}_{-0.29}$
0.22–0.40	$1.90^{+0.38}_{-0.30}$
0.40–0.60	$1.72^{+0.35}_{-0.27}$

case shows that it would be permissible to ignore the errors σ_i completely, i.e., our signal-to-noise ratio is high enough that we have "error-free data" (cf. Fig. 2). We have not done so in this paper, however.

The second comment is on the applicability of equation (2) to small samples. This equation is correct only in the limit of a "large" sample size. We have made simulations of our procedure to determine β for our worst case, the high-z sample containing five objects. We assumed that the luminosity function had a slope $\beta_{true} = 1.85$. From this distribution a set of five clusters was drawn at random, and the luminosities were modified by Gaussian fluctuations with sigmas similar to those in the actual observations. The slope, β_{est}, was determined using the standard procedure and the process repeated 500 times. The resulting histogram of β_{est} is shown in Figure 2. The most likely value of β was 1.75 compared with a β_{true} of 1.85. The range of β_{est} containing 68% of the estimates was 1.40–2.20, whereas the range given by equation (2) would be 1.45–2.07. We conclude that using equation (2) will slightly underestimate the error bounds but not by enough to warrant more extensive simulations. As a matter of interest, the dashed histogram in Figure 2 shows the results of identical simulations

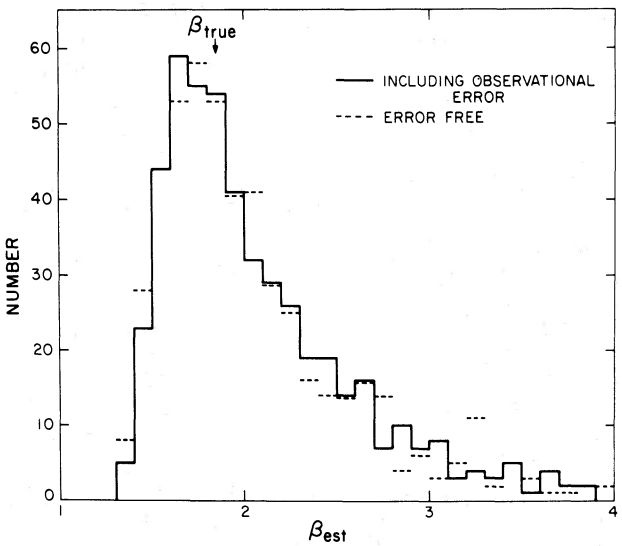

FIG. 2.—Histogram of the estimated X-ray luminosity function slope determined from 500 simulations similar to the high-z sample. The solid line includes observational error, the dashed lines are for the case of zero observational error. The two distributions are virtually identical.

except that the observational errors were set to zero. The two distributions are almost identical, which indicates that the influence of observational errors on estimates of β is minimal if we use observations with a signal-to-noise ratio greater than 4, as we are doing here.

Our final sample consists of the 25 clusters marked with an asterisk in Table 1. All but six are Abell clusters, and all but three are optically selected. These three are the clusters around 3C 295, 3C 19, and PKS 0116+08. The 3C 295 cluster is a richness class 1 cluster (Mathieu and Spinrad 1981) and would have been in Abell's list if it were closer. The 3C 19 cluster has been described by Kristian, Sandage, and Katem (1974) as containing "many faint galaxies," while the PKS 0116+08 cluster has been described by Spinrad *et al.* (1976) as a "rather rich cluster." It is probable that all the objects in our final sample are rich Abell-like clusters and are drawn from the same population studied previously at low redshift. Unfortunately, the luminosities of the three most distant detected clusters, near $z = 0.8$, could only be measured at the 3 σ level for the longest practical exposure. Thus these clusters are not in the statistical sample.

For comparison of our data with that for nearby clusters, we used the results from the *HEAO 1* A-2 survey by McKee *et al.* (1980). This sample is flux (not luminosity) limited and optically complete roughly to $z = 0.1$. In order to estimate the XLF slope in a manner as close as possible to that used for our distant samples, which are luminosity limited, we selected clusters with luminosities greater than 1.75×10^{44} ergs s^{-1}, redshifts less than 0.06 (which, for a limiting flux of 0.7 R15, introduces a luminosity threshold of 2.7×10^{44} ergs s^{-1}), and signal-to-noise ratio greater than 4. The objects satisfying these limits were used to obtain a maximum-likelihood estimation of the slope, which was $1.99^{+0.38}_{-0.31}$. This is consistent with the value of $2.18^{+0.32}_{-0.48}$ derived by McKee *et al.* (1980) (as corrected by Hintzen, Scott, and McKee 1980) for their total sample and with the value of 2.03 ± 0.18 derived by Piccinotti *et al.* (1982). These data are background limited so our neglect of the l_i dependence of σ_i is appropriate.

Within uncertainties, the available material does not demand strong evolution of the XLF slope with redshift. To find quantitative estimates for the evolution rate which is implied from Figure 1, we assumed a linear relation between β and z: $\beta = a + bz$. To find a and b, the maximum-likelihood technique was again applied. We constructed the likelihood function $L(a, b)$ by substituting for β in equation (1). The product now extends over all the clusters in the sample including those from the *HEAO 1* A-2 survey; thus this is not a small sample and equation (2) is applicable. The function S was minimized with respect to both a and b. The minimum was found for $a = 2.02$ and $b = -0.58^{+0.90}_{-0.85}$, clearly consistent with no evolution. This relation is shown by the line labeled "best fit" in Figure 1 and implies a limit on the time scale for slope changes, $|\tau_\beta| \equiv |(d\beta/dt)^{-1}| = b^{-1}H_0^{-1}|$ for $z = 0$ and $\Omega = 0$, of greater than 9×10^9 yr $(H_0/50)^{-1}$ at the 95% confidence level. We choose to parameterize our results in this way because both positive and negative values of τ_β are allowed by our data, and in particular an arbitrarily large value is allowed ($b = 0$).

There are some types of evolution which would not exhibit XLF slope changes. Examples of these would be pure luminosity evolution, where the luminosities of all objects vary with time by the same factor; or a dynamic evolution, where the luminosity of clusters continually increases with time because of gravitational contraction, but new low-luminosity clusters are continually virializing to fill the vacated luminosity interval. In these cases the shape of the XLF could be preserved even though the cluster population is evolving. In fact, Perrenod and Henry (1981) have presented evidence that the X-ray temperatures of distant ($z \approx 0.4$) clusters are lower than nearby objects by about a factor of 2. If the temperatures of individual clusters are evolving, then it is to be expected that their luminosities will evolve also. Our failure to detect any change in the XLF slope may mean that clusters do evolve according to one of these pathological cases. In this connection it is interesting to note that the radio galaxy luminosity function does evolve such that the normalization changes by more than a factor of 10, yet the slope changes by less than 1 to a redshift of 0.5 (Katgert, de Ruiter and van der Laan 1979).

IV. COMPARISON WITH A SPECIFIC MODEL

The luminosity function calculated by Perrenod (1980), under the assumptions given in the Introduction, is (his eq. [44] with $g = 1$, i.e., constant gas mass fraction with z)

$$N(L, z) = N_0(1 + z)^3\Delta(L/L_0{}^*)^{-(1+\epsilon\alpha)} \times \exp\left[-\Delta^2(L/L_0{}^*)^{2\epsilon(1-\alpha)}\right], \quad (3)$$

where $\Delta = \delta_v(z)/\delta_v(0) \approx 1 + \Omega^{0.6}z$ is the ratio of the perturbation undergoing virialization at z to that doing so now; α is related to the index n of the power spectrum of density perturbations at recombination, $\delta_k{}^2 \propto k^n$, by $\alpha = 1/2 - n/6$; ϵ is the index relating the X-ray luminosity to the cluster mass, $M \propto L^\epsilon$; and $L_0{}^*$ and N_0 are parameters of the model fixed by observation at $z = 0$. We will consider two simple cases for α. White noise is described by $n = 0$, $\alpha = 1/2$, while $n = -1$, $\alpha = 2/3$ is the simplest spectrum predicted by the standard big-bang cosmology (Gott and Rees 1975). Gott and Turner (1977) have found that $\alpha = 0.72 \pm 0.05$ fits their multiplicity function data. However, N-body simulations (Gott, Turner, and Aarseth 1979) imply that either power can match the observed galaxy covariance function depending on Ω. We also will consider two cases for ϵ: $\epsilon = 2/7$ and $\epsilon = 2/5$. Mushotzky *et al.* (1978) find that their observations of low-z clusters imply a value of 2/7 for ϵ with an error of about 0.04 (i.e., $\epsilon = 0.29 \pm 0.04$). We will only consider the four combinations given above and will not perform a detailed parameter estimation when fitting our data. We do this because our data are not sufficient to greatly

constrain these parameters (see below), and the model may be incorrect. In particular, Bhavsar (1980) has shown that a power-law distribution of fluctuations in the density enhancement about its mean (and not a Gaussian as assumed in the model) better explains the observed group fraction versus surface density enhancement data.

We have fitted equation (3) with N_0 and L_0^* as free parameters to the XLF of McKee *et al.* (1980) for the four possible combinations of α and ϵ given by $\alpha = 1/2$ or 2/3 and $\epsilon = 2/7$ or 2/5. All four fits are acceptable with $\chi_\nu^2 \approx 0.8$. For $\alpha = 1/2$ and $\epsilon = 2/7$, the best fit values are $\log N_0[\mathrm{Gpc}^{-3}(10^{44}\ \mathrm{ergs\ s}^{-1})^{-1}] = 4.49^{+1.16}_{-1.79}$ and $L_0^* = 0.085^{+0.745}_{-0.059} \times 10^{44}$ ergs s^{-1}. The errors are $\pm 1\ \sigma$. The best fit values of N_0 and L_0^* can vary by as much as a factor of 10 in either direction when α and ϵ take on the values given above.

Equation (3) can be transformed to

$$N(L, z) = N_0(1+z)^3\Delta^{(1+\epsilon)/\epsilon(1-\alpha)}[L/L^*(z)]^{-(1+\epsilon\alpha)} \times \exp\{-[L/L^*(z)]^{2\epsilon(1-\alpha)}\}, \quad (4)$$

where the characteristic luminosity at any epoch, $L^*(z)$, is

$$L^*(z) = L_0^*\Delta^{1/\epsilon(\alpha-1)} \approx L_0^*(1+\Omega^{0.6}z)^{1/\epsilon(\alpha-1)}. \quad (5)$$

In a manner similar to the previous section, we can determine $L^*(z)$ and its error for each distance bin. These values are plotted in Figure 3 for the model given by $\alpha = 1/2$, $\epsilon = 2/7$. We have also plotted equation (5) for several values of Ω. Low values of Ω are clearly favored. All other choices of α and ϵ gave very similar results.

Within the context of this specific model, we can determine the probability that Ω is less than 1. For the four models given by $\epsilon = 2/7$ or 2/5 and $\alpha = 1/2$ or 2/3, we find the $\Omega < 1$ at the 92% confidence level. For this calculation we have converted the observed fluxes to luminosities assuming $\Omega = 1$. This is conservative, assuming $\Omega = 0$ for the luminosity conversion results in an even higher probability that $\Omega < 1$.

Finally, we have determined a quantitative limit on the time scale of evolution of L^* by assuming $\log L_{44}^*(z) = a + bz$, where $L_{44}^*(z)$ is the value of $L^*(z)$ in units of 10^{44} ergs s^{-1}. We constructed the likelihood function from all the data in a similar manner as in the last section to determine the one interesting parameter, b. For a wide range of α, ϵ, and Ω, the value of b was relatively constant. For $\alpha = 1/2$, $\epsilon = 2/7$, and $\Omega = 0$, $b = 1.22^{+2.02}_{-1.87}$, which is representative of all the models considered. This implies that $\tau_{L^*} \equiv |1/L^* \cdot dL^*/dt|^{-1} = |2.3/b \cdot dt/dz| = |(2.3/b)H_0^{-1}|$ at $z = 0$ for $\Omega = 0$. So τ_{L^*} is greater than 8.5×10^9 yr $(H_0/50)^{-1}$ at the 95% confidence level. The same quantity for first-ranked cluster galaxies, if $\Omega = 0$, is approximately $+1.3 \times 10^{10}$ yr (Kristian, Sandage, and Westphal 1978).

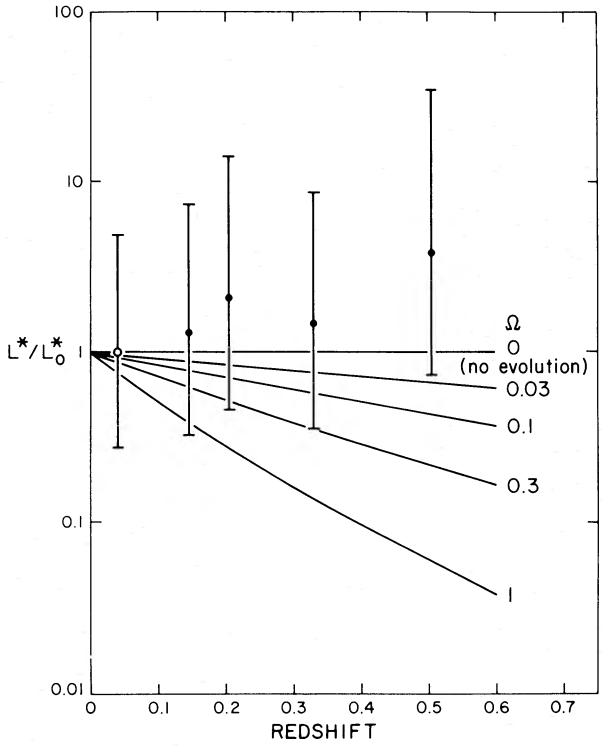

FIG. 3.—The ratio of the characteristic cluster X-ray luminosity at a given epoch to that at the present epoch. Symbols are the same as in Fig. 1. The lines are eq. (5) with $\alpha = 1/2$ and $\epsilon = 2/7$ for the value of Ω indicated.

We thank B. Dennison for communicating the luminosity of A963 before publication. A. S. thanks R. Giacconi for his hospitality at CfA. Some of the calculations reported here were made with the PDP 11/45 computer donated to the N. Copernicus Astronomical Center by the US National Academy of Sciences, following the initiative and through the action of Dr. C. R. O'Dell and Mr. A. M. Baer. J. P. H. wishes to thank one of his coauthors for substantial contributions to this paper made under very difficult circumstances. This work was supported by NASA contract NAS 8-30751.

REFERENCES

Ayni, Y., Soltan, A., Tananbaum, H., and Zamorani, G. 1980, *Ap. J.*, **238**, 800.
Bahcall, N. A. 1977, *Ap. J. (Letters)*, **217**, L77.
Bhavsar, S. U. 1980, *Ap. J.*, **237**, 671.
Boynton, P., Radford, S., Schommer, R., and Murray, S. 1982, *Ap. J.*, **257**, 473.
Butcher, H., Oemler, A., and Wells, D. 1980, in *IAU Symposium 92, Objects of High Redshifts*, ed. G. A. Abell and P. J. E. Peebles (Dordrecht: Reidel), p. 49.
Cash, W. 1979, *Ap. J.*, **228**, 939.
Crawford, D. F., Jauncey, D. L., and Murdoch, H. S. 1970, *Ap. J.*, **162**, 405.
Fall, S. M. 1979, *Rev. Mod. Phys.*, **51**, 21.
Gott, J. R., III, and Rees, M. J. 1975, *Astr. Ap.*, **45**, 365.
Gott, J. R., III, and Turner, E. L. 1977, *Ap. J.*, **216**, 357.
Gott, J. R., III, Turner, E. L., and Aarseth, S. J. 1979, *Ap. J.*, **234**, 13.
Helfand, D. J., Ku, W. H. M., and Abramopoulos, F. 1980, *Highlights of Astronomy*, **5**, 747.

Henry, J. P., Branduardi, G., Briel, U., Fabricant, D., Feigelson, E., Murray, S., Soltan, A., and Tananbaum, H. 1979, *Ap. J.* (*Letters*), **234**, L15.
Hintzen, P., Scott, J. S., and McKee, J. D. 1980, *Ap. J.*, **242**, 857.
Jones, C., and Forman, W. 1978, *Ap. J.*, **224**, 1.
Katgert, P., de Ruiter, H. R., and van der Laan, H. 1979, *Nature*, **280**, 20.
Koo, D. C. 1981, *Ap. J.* (*Letters*), **251**, L75.
Kristian, J., Sandage, A., and Katem, B. N. 1974, *Ap. J.*, **191**, 43.
Kristian, J., Sandage, A., and Westphal, J. A. 1978, *Ap. J.*, **221**, 383.
Lebofsky, M. J. 1981, *Ap. J.* (*Letters*), **245**, L59.
Lightman, A. P., Hertz, P., and Grindlay, J. E. 1980, *Ap. J.*, **241**, 367.
Mathieu, R. D., and Spinrad, H. 1981, *Ap. J.*, **251**, 485.
McHardy, I. 1978, *M.N.R.A.S.*, **184**, 783.
McKee, J. D., Mushotzky, R. F., Boldt, E. A., Holt, S. S., Marshall, F. E., Pravdo, S. M., and Serlemitsos, P. J. 1980, *Ap. J.*, **242**, 843.
Murdoch, H. S., Crawford, D. F., and Jauncey, D. L. 1973, *Ap. J.*, **183**, 1.
Mushotzky, R. F., Serlemitsos, P. J., Smith, B. W., Boldt, E. A., and Holt, S. S. 1978, *Ap. J.*, **225**, 21.
Perrenod, S. C. 1980, *Ap. J.*, **236**, 373.
Perrenod, S. C., and Henry, J. P. 1981, *Ap. J.* (*Letters*), **247**, L1.
Piccinotti, G., Mushotzky, R. F., Boldt, E. A., Holt, S. S., Marshall, E. E., Serlemitsos, P. J., and Shafer, R. A. 1982, *Ap. J.*, **253**, 485.
Pravdo, S. H., Boldt, E. A., Marshall, F. E., McKee, J., Mushotzky, R. F., Smith, B. W., and Reichert, G. 1979, *Ap. J.*, **234**, 1.
Schwartz, D. A. 1978, *Ap. J.*, **220**, 8.
Spinrad, H., Liebert, J., Smith, H. E., and Hunstead, R. 1976, *Ap. J.* (*Letters*), **206**, L79.
Spinrad, H., Stauffer, J., and Butcher, H. 1981, *Ap. J.*, **244**, 382.
Ulmer, M. P., *et al.* 1980, *Ap. J.*, **235**, 351.
Ulmer, M. P., *et al.* 1981, *Ap. J.*, **243**, 681.

ULRICH BRIEL: Max-Planck-Institut für Physik und Astrophysik, Institut für extraterrestrische Physik, 8046 Garching, West Germany

JAMES E. GUNN: Princeton University Observatory, Peyton Hall, Princeton, NJ 08540

J. PATRICK HENRY: Institute for Astronomy, 2680 Woodlawn Drive, Honolulu, HI 96822

ANDRZEJ SOLTAN: N. Copernicus Astronomical Center, Bartycka 18, 00-716 Warsaw, Poland